magnetochemistry

MDPI

Article

Heterobimetallic One-Dimensional Coordination Polymers $M^{I}Cu^{II}$ (M = Li and K) Based on Ferromagnetically Coupled Di- and Tetracopper(II) Metallacyclophanes

Tamyris T. da Cunha [1], Willian X. C. Oliveira [1], Emerson F. Pedroso [2], Francesc Lloret [3], Miguel Julve [3] and Cynthia L. M. Pereira [1,*]

1 Departamento de Química, Instituto de Ciências Exatas, Universidade Federal de Minas Gerais, Av. Antônio Carlos 6627, Pampulha, Belo Horizonte, Minas Gerais 31270901, Brazil; tamyris.cunha@gmail.com (T.T.d.C.); williancoliveira@yahoo.com.br (W.X.C.O.)

2 Centro Federal de Educação Tecnológica de Minas Gerais, Av. Amazonas 5855, Belo Horizonte, Minas Gerais 30421169, Brazil; pedroso@cefetmg.br

3 Departamento de Química Inorgánica/Instituto de Ciencia Molecular (ICMol), Universitat de València, C/ Catedrático José Beltrán 2, 46980 Paterna (València), Spain; Francisco.Lloret@uv.es (F.L.); Miguel.Julve@uv.es (M.J.)

* Correspondence: cynthialopes@ufmg.br; Tel.: +55-31-3409-7556

Received: 17 July 2018; Accepted: 16 August 2018; Published: 25 August 2018

Abstract: The synthesis, crystal structure and magnetic properties of the coordination polymers of formula $[EDAP\{Li_6(H_2O)_8[(Cu_2(\mu\text{-mpba})_2)_2(H_2O)_2]\}]_n$ (**1**) and $[(EDAP)_2\{K(H_2O)_4[Cu_2(\mu\text{-mpba})_2(H_2O)_2]\}Cl{\cdot}2H_2O]_n$ (**2**), in which mpba = *N*,*N*′-1,3-phenylenebis(oxamate) and $EDAP^{2+}$ = 1,1′-ethylenebis(4-aminopyridinium) are described. Both compounds have in common the presence of the $[Cu_2(mpba)_2]^{4-}$ tetraanionic unit which is a [3,3] metallacyclophane motif in which the copper(II) ions are five-coordinate in a distorted square pyramidal surrounding. The complex anion in **1** is dimerized through double out-of-plane copper to outer carboxylate-oxygen atoms resulting in the centrosymmetric tetracopper(II) fragment $[Cu_4(\mu\text{-mpba})_4(H_2O)_2]^{8-}$ which act as a ligand toward six hydrated lithium(I) cations leading to anionic ladder-like double chains whose charge is neutralized by the $EDAP^{2+}$ cations. In the case of **2**, each dicopper(II) entity acts as a ligand towards tetraquapotassium(I) units to afford anionic zig zag single chains of formula $\{K(H_2O)_4[Cu_2(\mu\text{-mpba})_2(H_2O)_2]\}_n^{3n-}$ plus $EDAP^{2+}$ cations and non-coordinate chloride anions. Cryomagnetic measurements on polycrystalline samples **1** and **2** show the occurrence of ferromagnetic interactions between the copper(II) ions across the $-N_{amidate}-(C-C-C)_{phenyl}-N_{amidate}-$ exchange pathway [J = +10.6 (**1**) and +8.22 cm^{-1} (**2**)] and antiferromagnetic ones through the double out-of-plane carboxylate-oxygen atoms [$j = -0.68$ cm^{-1} (**1**), the spin Hamiltonian being defined as $\boldsymbol{H} = -J(\boldsymbol{S}_{Cu1}\cdot\boldsymbol{S}_{Cu2} + \boldsymbol{S}_{Cu2^i}\cdot\boldsymbol{S}_{Cu1^i}) - j(\boldsymbol{S}_{Cu2}\cdot\boldsymbol{S}_{Cu2^i})$].

Keywords: oxamate; copper(II); crystal engineering; spin polarization; ferromagnetic coupling; coordination polymers

1. Introduction

Nowadays molecular magnetism has become an interdisciplinary field in which scientists of different domains such as organic and inorganic chemistry, physical chemistry, condensed matter physics and biology have invested impressive research efforts. This diversity has led to a fast and significant progress of the different approaches of molecular magnetism, which depends on the nature of the spin carriers, these ones being organic radicals and/or paramagnetic metal ions [1,2].

Over the last two decades, research involving tetranuclear compounds has provided us with better mathematical models and accurate interpretations of the magnetic behaviors [3–8] even including magneto-structural correlations [9–11]. In this direction, the design of the ligand is not only the first step but a crucial choice in the self-assembly of metal ions resulting in coordination compounds with predictable magnetic properties. Combining the versatility of the oxamate as a bridge and the aromaticity of the deprotonated form of the *N*,*N*′-1,3-phenylenebis(oxamic acid) molecule (hereafter noted H_4mpba), a moderate ferromagnetic coupling between two copper(II) ions in the dinuclear metallacyclophane $Na_4[Cu_2(\mu\text{-mpba})_2]\cdot 10H_2O$ (J = +16.8 cm^{-1}) [12] was achieved the intramolecular copper-copper separation being ca. 6.8 Å. High-nuclearity homometallic compounds with transition metal ions and mpba ligands were synthesized in a programmed stepwise manner such as the octanuclear copper(II) complex $Na_2\{[Cu_2(\mu\text{-mpba})_3][Cu(pmdien)]_6\}(ClO_4)_6\cdot 12H_2O$ (pmdien = *N*,*N*,*N*′,*N*″, *N*″-pentamethyldiethylenetriamine) and the octanickel(II) species $\{[Ni_2(\mu\text{-mpba})_3][Ni(dpt)(H_2O)]_6\}(ClO_4)_4\cdot 12.5H_2O$ [13] (dpt = dipropylenetriamine). Both compounds exhibit "dimer of tetramers" structures, with two oxamate-bridged propeller shaped tetranuclear units connected through three *meta*-substituted phenylenediamidate bridges. Overall, antiferro- and ferromagnetic behaviors for the octacopper(II) and octanickel(II) complexes were observed, respectively, with an appreciable magnetic anisotropy in this latter case.

Besides the possibility of self-assembled structures, the use of the mpba ligand with its variety of coordination modes allows the generation of supramolecular structures exhibiting different dimensionalities (nD with n = 2 and 3) [14,15]. Illustrative examples are brick-wall-like 2D motifs assembled from $[Cu_2(\mu\text{-mpba})_2]^{4-}$ in $[\{Cu_2(\mu\text{-mpba})_2\}Cu_2(H_2O)_8]\cdot 6H_2O$ [16] and in $[Co_2Cu_2(\mu\text{-mpba})_2(H_2O)_6]\cdot 6H_2O$ [17], honeycomb 3D networks $Li_5[Li_3Ni_2(\mu\text{-mpba})_3(H_2O)_6]\cdot 31H_2O$ and $Li_5[Li_3Co_2(\mu\text{-mpba})_3(H_2O)_6]\cdot 31H_2O$ also called MOCNs (Metal–Organic Coordination Networks) which behave as rather well-isolated M_2^{II} (M = Ni and Co) dimers with a moderate to weak ferromagnetic coupling [18], and the chiral hexagonal supramolecular 3D network $(HNEt_3)_2[Co_2(\mu\text{-}H_2mpba)_3]\cdot 6DMF\cdot 5H_2O$ [19] ($HNEt_3^+$ = triethylammonium cation) obtained by solvothermal synthesis, for instance.

The intense research in materials science and nanotechnology also reached the molecular-based magnets, now designing them as multifunctional molecular materials. MOCNs based on the mpba ligand [20] have already been applied as solid-state anion–host for encapsulation [21], reversible solvatomagnetic switching [22] acting as selective magnetic adsorbent for gas and vapor [23] and 3D porous coordination polymers [24].

More recently, oxamate-based compounds with higher nuclearity were prepared using two different strategies. One of them consists of the combination of the mpba ligand and first- or second-row transition metal ions described as "dimer of trimers" in which two $Cu^{II}-Pd^{II}-Cu^{II}$ trinuclear units are connected by two mpba ligands [25]. The other one was the organic counterion modulated strategy in metathesis reactions with different $(cat)_2[Cu(opba)]$ [H_4opba = *N*,*N*′-1,2-phenylenediaminebis (oxamic acid)] building blocks resulting in dimers of Cu^{II} arranged in supramolecular chains [26]. Dealing with this last bis(oxamic) acid, some of its compounds have interesting catalytic properties and exhibit single-crystal-to single-crystal phase transitions [27–30].

Having in mind all those achievements with oxamate-based compounds, we decided to unite the possibility to play with supramolecular chemistry using the organic counterion $EDAP^{2+}$ [$EDAP^{2+}$ = 1,1′-ethylenebis(4-aminopyridinium)] featuring many sites of intermolecular interactions and the coordination versatility of the anionic $[Cu_2(\mu\text{-mpba})_2]^{4-}$ building block toward alkaline metal ions seeking out the synthesis of coordination polymers of varying dimensionalities and topologies (Scheme 1). In the following, we present the first results which concern the preparation, structural characterization and cryomagnetic investigation of the heterobimetallic compounds of formula $[EDAP\{Li_6(H_2O)_8[(Cu_2(\mu\text{-mpba})_2)_2(H_2O)_2]\}]_n$ (**1**) and $[(EDAP)_2\{K(H_2O)_4[Cu_2(\mu\text{-mpba})_2(H_2O)_2]\}Cl\cdot 2H_2O]_n$ (**2**).

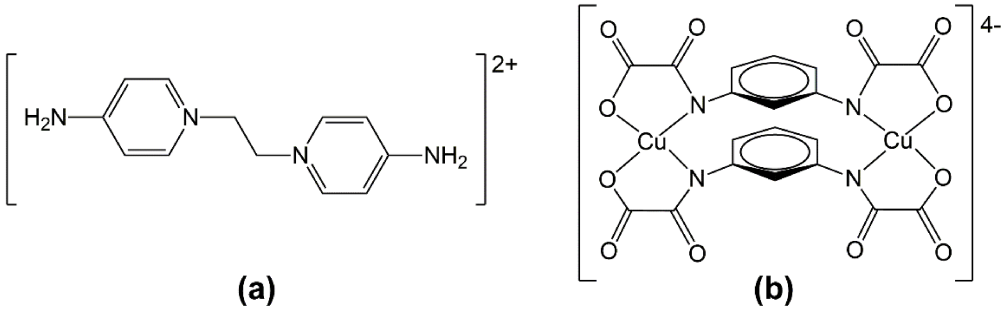

Scheme 1. Molecular structure of the (**a**) $EDAP^{2+}$ cation and (**b**) $[Cu_2(\mu\text{-mpba})_2]^{4-}$ building block.

2. Materials and Methods

2.1. Starting Materials

The reagents and solvents were purchased from Sigma Aldrich and they were used as received. The diethyl ester form of the mpba ligand (Et_2H_2mpba proligand) and the $(EDAP)Cl_2{\cdot}2H_2O$ salt were synthesized by following previously reported methods [12,26]. Elemental analyses (C, H and N) were performed with a Perkin-Elmer 2400 elemental analyzer. The lithium and copper contents were determined by atomic absorption spectrometry with a Hitachi Z-8200 Polarized Atomic Absorption Spectrophotometer. Infrared spectra were recorded on a Perkin Elmer 882 spectrophotometer in the range 4000 and 400 cm^{-1} using dry KBr pellets. Thermal analyses (TG curves) of **1** and **2** were carried in alumina crucibles sample holing on a Shimadzu TGA-60 using dynamic nitrogen atmosphere (see Supplementary Information, Figures S1 and S2). X-ray diffraction patterns for **1** and **2** were obtained by means of a Rigaku/eirgeflex diffractometer working at room temperature. Diffraction data were collected in the Bragg/Brentano mode ($deg{\cdot}s^{-1}$) using monochromatic Cu-Kα radiation (see Supplementary Information, Figures S3 and S4).

*2.2. Synthesis of $[EDAP\{Li_6(H_2O)_8[(Cu_2(\mu\text{-}mpba)_2)_2(H_2O)_2]\}]_n$ (**1**)*

Compound **1** was prepared by the one-step reaction of the Et_2H_2mpba proligand with copper(II) nitrate trihydrate and lithium(I) hydroxide (1:1:4.2 molar ratio) in water plus a further addition of $(EDAP)Cl_2{\cdot}2H_2O$. The detailed procedure is as follows: an aqueous solution (5 mL) of $Cu(NO_3)_2{\cdot}3H_2O$ (0.24 g, 1.0 mmol) was added dropwise to an aqueous solution (15 mL) of Et_2H_2mpba (0.308 g, 1.0 mmol) and $LiOH{\cdot}H_2O$ (0.167 g, 4.2 mmol) with stirring at room temperature. The resulting deep-green solution was filtered to discard any solid particle. Then, an aqueous solution (5 mL) of $(EDAP)Cl_2$ $\cdot 2H_2O$ (0.323 g, 1.0 mmol) was added dropwise and the pale green solution was left to crystallize at room temperature. X-ray quality green needles of **1** were grown after 3 days. The crystals were filtered and dried on filter paper at room temperature. Yield: 0.227 g, 54%. Anal. Calcd for $C_{52}H_{52}Cu_4Li_6N_{12}O_{34}$ (**1**): C, 37.07; H, 3.11; N, 9.98; Cu, 15.09; Li, 2.47. Found: C, 37.21; H, 3.22; N, 10.14, Cu, 15.06; Li, 2.37. IR (KBr, cm^{-1}): 3422 (O−H), 3172 (N−H), 1657, 1600 (C=O), 1483 (C=C), 1340 (C−O), 1208 (C−N), 840, 828 (C−H) cm^{-1}.

*2.3. Synthesis of $[(EDAP)_2\{K(H_2O)_4[Cu_2(\mu\text{-}mpba)_2(H_2O)_2]\}Cl{\cdot}2H_2O]_n$ (**2**)*

Compound **2** was prepared by the one-step reaction of the corresponding Et_2H_2mpba proligand with copper(II) nitrate and potassium hydroxide (1:1:4.2 molar ratio) in water with further addition of $(EDAP)Cl_2{\cdot}2H_2O$. The detailed procedure is as follows: an aqueous solution (5 mL) of $Cu(NO_3)_2{\cdot}3H_2O$ (0.24 g, 1.0 mmol) was added dropwise to an aqueous solution (15 mL) of Et_2H_2mpba (0.308 g, 1.0 mmol) and KOH (0.235 g, 4.2 mmol) with stirring at room temperature and the resulting deep-green solution was filtered to discard any solid particle. Then, an aqueous solution (5 mL) of $(EDAP)Cl_2$ $2H_2O$ (0.323 g, 1.0 mmol) was added dropwise. Green needles of **2** suitable for X-ray experiments separated from the resulting pale green solution on standing at room temperature after several days.

The crystals were filtered and dried under ambient conditions. Yield: 0.291 g, 47%. Anal. Calcd for $C_{44}H_{56}ClCu_2KN_{12}O_{20}$ (**2**): C, 41.46; H, 4.43; N, 13.19; Cu, 9.97. Found: C, 42.31; H, 4.36; N, 13.34, Cu, 9.99%. IR (KBr, cm^{-1}): 3435 (O−H), 3123 (N−H), 1674, 1641 (C=O), 1489 (C=C), 1313 (C−O), 1228 (C−N), 859 (C−H) cm^{-1}.

2.4. Crystallographic Data Collection and Refinement

Single crystal X-ray diffraction data were collected on an Oxford-Diffraction GEMINI-Ultra diffractometer (LabCri) at 150 K using Mo Kα radiation (λ = 0.71073 Å). The program *CrysAlisPro* [31] was used for data integration, scaling of the reflections and analytical absorption corrections. Final unit cell parameters were based on the fitting of all reflections positions. Non-merohedral twinning was observed for both compounds and the data were treated using also *CrysAlisPro* with two domains. The space group identification was done with XPREP [32] and the crystal structures were solved with direct methods with SIR-92 [33]. The refinements were performed using SHELXL2018 [34] based on F^2 through full-matrix least-squares routine, using the WinGX [35] graphical user interface. All non-hydrogen atoms, except for the disordered ones, were refined anisotropically, and the hydrogen atoms were placed at calculated positions and refined isotropically with a riding model. Disordered atoms, except for those from crystallization water molecules in both structures, were split into two positions with occupancy refined independently for each disordered moiety. The crystallization water molecules were placed in electronic maxima not bonded to the rest of the structure with free refined occupancy. A summary of the crystal data, experimental details, and refinement results for **1** and **2** is given in Table 1 in which whereas selected bond lengths and angles are grouped in Table 2 (**1**) and Table 3 (**2**). Crystallographic data for the structures of **1** and **2** have been deposited at the Cambridge Crystallographic Data Centre with CCDC reference numbers 1846817 (**1**) and 1846818 (**2**).

Table 1. Summary of Crystallographic Data for **1** and **2**.

Compound	**1**	**2**
Formula	$C_{26}H_{16}N_6O_{21.48}Cu_2Li_3$	$C_{44}H_{52}ClCu_2KN_{12}O_{25.38}$
Fw/g mol^{-1}	903.96	1344.65
T/K	150	150
λ/Å	0.71073	0.71073
Crystal System	Triclinic	Monoclinic
Space group	$P\bar{1}$	$I2/a$
a/Å	9.3856 (5)	14.0948(7)
b/Å	10.3708 (6)	15.6318(11)
c/Å	19.3438(10)	27.4889(15)
α/°	92.925(4)	90
β/°	96.846(4)	102.879(5)
γ/°	98.239(4)	90
V/Å^3	1845.68(18)	5904.2(6)
Z	2	4
ρ/mg m^{-3}	1.627	1.513
μ/mm^{-1}	1.245	0.928
$F(000)$	906	2740
Crystal size/mm^3	0.40 × 0.17 × 0.10	0.38 × 0.13 × 0.11
Reflections collected (R_{int})	15068 (0.069)	13128 (0.113)
Unique Reflections	15068	13128
Reflections with $I \geq 2\sigma(I)$	10152	7712
Goodness-of-fit on F^2	1.426	1.173
R^a, wR^b	0.1218, 0.3603	0.0815, 0.2378
R^a, wR^b *(all data)*	0.1545, 0.3789	0.1219, 0.2539
Larg. diff. peak and hole/e Å^{-3}	3.268, −1.073	1.907, −0.952

$^a R = \Sigma \, | \, |F_o| - |F_c| \, | \, / \Sigma |F_o|$. ^{b} wR $[\Sigma \, (|F_o|^2 - |F_c|^2)^2 / \Sigma |F_o|^2]^{1/2}$.

Table 2. Main Bond Lengths (Å) and Angles (deg) for **1** [a].

Bond Lengths/Å		Bond Angles/deg	
Cu1—N1	1.975 (6)	N1—Cu1—N2	104.2 (3)
Cu1—N2	1.977 (7)	N1—Cu1—O1	83.2 (5)
Cu1—O1	1.984 (16)	N1—Cu1—O4	162.6 (4)
Cu1—O4	2.056 (12)	N1—Cu1—O13	94.9 (3)
Cu1—O13	2.299 (7)	N2—Cu1—O1	162.1 (5)
Cu2—N3	1.953 (6)	N2—Cu1—O4	82.7 (4)
Cu2—N4	1.951 (6)	N2—Cu1—O13	97.8 (3)
Cu2—O7	1.978 (5)	O1—Cu1—O4	85.9 (6)
Cu2—O10	1.985 (5)	O1—Cu1—O13	97.8 (5)
Cu2—O10^{i}	2.682 (6)	O4—Cu1—O13	100.0 (5)
Li1—O8	2.113 (15)	N3—Cu2—N4	102.9 (2)
Li1—O9	2.007 (15)	N3—Cu2—O7	84.0 (2)
Li1—O11^{ii}	2.083 (15)	N3—Cu2—O10	170.7 (2)
Li1—O12^{ii}	2.006 (16)	N3—Cu2—O10^{i}	100.4 (2)
Li1—O19	2.083 (18)	N4—Cu2—O7	167.4 (2)
Li2—O2	2.04 (3)	N4—Cu2—O10	84.1 (2)
Li2—O3	2.08 (3)	N4—Cu2—O10^{i}	105.2 (2)
Li2—O5^{ii}	2.08 (3)	O7—Cu2—O10	88.0 (2)
Li2—O6^{ii}	2.06 (3)	O7—Cu2—O10^{i}	85.3 (2)
Li2—O14	2.09 (3)	O10—Cu2—O10^{i}	83.3 (2)
Li3—O3	1.77 (3)	O8—Li1—O9	81.1 (5)
Li3—O6^{ii}	1.88 (3)	O8—Li1—O11^{ii}	100.9 (7)
Li3—O17	1.80 (3)	O8—Li1—O12^{ii}	157.9 (9)
Li3—O15	2.05 (3)	O8—Li1—O19	100.5 (8)
		O9—Li1—O11^{ii}	154.6 (10)
		O9—Li1—O12^{ii}	87.0 (6)
		O9—Li1—O19	98.6 (7)
		O11^{ii} —Li1—O12^{ii}	82.1 (6)
		O11^{ii} —Li1—O19	105.9 (7)
		O12^{ii} —Li1—O19	99.7 (7)
		O2—Li2—O3	81.1 (11)
		O2—Li2—O5^{ii}	105.2 (13)
		O2—Li2—O6^{ii}	156.3 (16)
		O2—Li2—O14	97.1 (14)
		O3—Li2—O14	103.7 (14)
		O3—Li2—O6^{ii}	84.5 (12)
		O3—Li2—O5^{ii}	157.6 (16)
		O5^{ii}—Li2—O6^{ii}	81.8 (11)
		O5^{ii}—Li2—O14	97.0 (13)
		O6^{ii}—Li2—O14	104.5 (14)
		O3—Li3—O6^{ii}	85.9 (11)
		O3—Li3—O15^{ii}	127.5 (15)
		O17—Li3—O3	102.1 (13)
		O17—Li3—O6^{ii}	118.5 (15)
		O6^{ii}—Li3—O17	97.8 (12)
		O6^{ii}—Li3—O15	135.5 (15)
		O17—Li3—O15	101.6 (14)

[a] Symmetry code: (i) = $2 - x$, $1 - y$, $1 - z$; (ii) = x, $1 - y$, z.

Table 3. Main Bond Lengths (Å) and Angles (deg) for **2** [a].

Bond Lengths/Å		Bond Angles/deg	
Cu1—N1	1.975 (6)	N1—Cu1—N2^{i}	106.9 (3)
Cu1—N2^{i}	1.977 (7)	N1—Cu1—O1	83.6 (3)
Cu1—O1	1.984 (16)	N1—Cu1—O4^{i}	83.0 (3)
Cu1—O4^{i}	2.056 (12)	N1—Cu1—O7	95.0 (3)
Cu1—O7	2.55 (1)	N2^{i}—Cu1—O1	169.3 (2)
K1—O1	2.892 (6)	N2^{i} —Cu1—O4^{i}	83.0 (3)
K1—O4	2.799 (6)	N2^{i} —Cu1—O7	91.4 (3)
K1—O8	2.812 (9)	O1—Cu1—O4^{i}	86.4 (2)
K1—O9^{ii}	2.999 (7)	O1—Cu1—O7	89.4 (3)
		O4^{i}—Cu1—O7	86.0 (3)
		O1—K1—O1^{vi}	127.1 (3)
		O1—K1—O4	55.95 (16)
		O1—K1—O4^{vi}	101.75 (18)
		O1^{vi}—K1—O4	101.75 (18)
		O1^{vi}—K1—O4^{vi}	55.95 (16)
		O1—K1—O8	79.3 (2)
		O1—K1—O8^{vi}	147.1 (2)
		O1^{vi}—K1—O8	147.1 (2)
		O1^{vi}—K1—O8^{vi}	79.3 (2)
		O1^{vi}—K1—O9^{ii}	67.76 (18)
		O1—K1—O9^{ii}	131.30 (18)
		O1^{vi}—K1—O9^{iii}	131.30 (18)
		O1—K1—O9^{iii}	67.75 (18)
		O4^{vi}—K1—O4	132.8 (3)
		O4—K1—O8	75.8 (3)
		O4—K1—O8^{vi}	146.4 (3)
		O4^{vi}—K1—O8	146.4 (3)
		O4^{vi}—K1—O8^{vi}	75.8 (3)
		O4—K1—O9^{ii}	76.38 (19)
		O4—K1—O9^{iii}	119.24 (17)
		O4^{vi}—K1—O9^{ii}	119.23 (17)
		O4^{vi}—K1—O9^{iii}	76.38 (19)
		O8—K1—O8^{vi}	85.5 (4)
		O8—K1—O9^{ii}	80.0 (3)
		O8—K1—O9^{iii}	73.1 (3)
		O8^{vi}—K1—O9^{ii}	73.1 (3)
		O8^{vi}—K1—O9^{iii}	80.0 (3)
		O9^{ii}—K1—O9^{iii}	143.2 (3)

[a] Symmetry code: (i) = $5/2 - x, y, 2 - z$; (ii) = $2 - x, -y, 2 - z$; (iii) = $1/2 - x, -y, z$; (iv) = $2 - x, 1/2 - y, 3/2 - z$; (v) = $2 - x, 1 - y, 2 - z$; (vi) = $3/2 - x, y, 2 - z$; (vii) = $2 - x, 1/2 + y, 3/2 - z$.

2.5. Magnetic Measurements

The magnetic susceptibility measurements were carried out on crushed single crystals of **1** and **2** in the temperature range 2.0–300 K with a Quantum Design SQUID magnetometer and using applied magnetic fields of 0.5 T ($T \geq 100$ K) and 1000 G ($2.0 \leq T < 100$ K). Diamagnetic corrections of the constituent atoms were estimated from Pascal's constants [36] as -749×10^{-6} (**1**) and -620×10^{-6} cm^3 mol^{-1} (**2**) [per two copper(II) ions in both cases]. Corrections for the temperature-independent paramagnetism [60×10^{-6} cm^3·mol^{-1} per copper(II) ion] and for the magnetization of the sample holder (a plastic bag) were also applied.

3. Results and Discussion

3.1. Description of the Crystal Structures of ***1*** *and* ***2***

Compound **1** crystallizes in the triclinic space group $P\bar{1}$, with the asymmetric unit composed by a dicopper(II) $[Cu_2(\mu\text{-mpba})_2]^{4-}$ unit (Figure 1a), in which three lithium(I) cations are coordinated to it. In order to reach the charge balance, half of $EDAP^{2+}$ cation appears in this asymmetric unit together with coordinated water molecules to the lithium(I) cations. The two copper(II) ions of the dinuclear fragment (Cu1 and Cu2) are coordinated to two oxamate groups from two $mpba^{4-}$ ligands in a bidentate form. Due to the geometrical constraints of this ligand, it cannot adopt the tetradentate coordination mode observed in its parent ligand in which the two oxamate substituents are in *ortho* position; however, a *cis*-CuN_2O_2 coordination sphere occurs in relation to the bidentate oxamate groups. The resulting [3,3] metallacyclophane-type motif of this dicopper(II) entity is also somewhat driven by π-stacking between the phenyl groups of the two mpba ligands which are placed very close (h = 3.38 Å between the geometric centers) and almost parallel [θ = 10.7(1)° from mean planes] to each other. The value of the dihedral angle between the basal planes of the copper atoms (Φ) is 59.2(2)° and the intermetallic distance (r) is equal to 7.030(1) Å. All these values are slightly different from those in the compound $Na_4[Cu_2(\mu\text{-mpba})_2]\cdot 10H_2O$ [12] (h = 3.36 Å, θ = 7.5°, Φ= 58° and r = 6.822 Å, respectively). Cu1 and Cu2 are five-coordinate in somewhat distorted square pyramidal surroundings. Their basal planes are defined by the O1N1N2O4 (Cu1) and O7N3N4O10 (Cu2) sets of atoms whereas the apical sites are filled by a water molecule (O13 at Cu1) and a carboxylate-oxygen from an oxamate group of an adjacent $[Cu_2(\mu\text{-mpba})_2]^{4-}$ unit [$O10^{i}$ at Cu2; symmetry code: (i) = $2-x$, $1-y$, $1-z$]. The copper atoms are shifted from the mean basal plane by 0.261 (Cu1) and 0.135 Å (Cu2) towards the apical position. The values for the trigonality parameter (τ) are equal to 0.015 (Cu1) and 0.057 (Cu2) (τ = 0 and 1 for ideal square pyramidal and trigonal bipyramidal, respectively) [37].

This unusual coordination mode for *meta*-substituted bis-oxamate ligand in **1** is reported here for the first time, despite it has been already described for *ortho* [26,38,39] and *para* [40] derivatives. It is important to point out that several counterions were used to obtain $[Cu_2(\mu\text{-mpba})_2]^{4-}$ complexes in the literature such as Na^+ [12], Li^+ [41,42], methylviologen (MV^{2+}) [43] 1-alkyl-3-methylimidazolium $[C_4MIm]^+$ [44] and (*S*)-1-phenylethyl-trimethylammonium $[(S)\text{-(1-PhEt)Me}_3N]^+$ [45] for instance, as described in the literature. In these cases, the resulting structures were composed by the [3,3] metallacyclophane-type motif of dicopper(II) ions in a dinuclear entity containing mpba as ligand. The $EDAP^{2+}$ dication combined with Li^+ ions in the presence of the metallacyclophane $[Cu_2(\mu\text{-mpba})_2]^{2-}$ moiety led to the tetranuclear copper(II)-oxamate unit, compound **1**, which is the unique tetracopper(II) example reported in the literature so far. Besides that, it has already been shown that the $EDAP^{2+}$ cation as an additional templating counterion is justified by its ability to establish both hydrogen bonds and $\pi-\pi$ interactions in the solid state due to the presence of the amino substituents at the pyridinium aromatic rings [26].

This dimerization of the $[Cu_2(\mu\text{-mpba})_2]^{4-}$ units turns into a centrosymmetric tetracopper(II) entity (Figure 1b) with metal-metal distances of 15.166(2), 8.472(1) and 3.517(1) Å for $Cu1\cdots Cu1^{i}$, $Cu1\cdots Cu2^{i}$ and $Cu2\cdots Cu2^{i}$, respectively. It should be noted that the value of the copper to apical oxygen atom bond length in this out-of-plane coordination [2.683(1) Å for $Cu2–O10^{i}$] is longer than the apical copper to water [Cu1–O13 = 2.297(1) Å] probably due to steric effects in the assembling of the two dicopper(II) entities. The angle at the bridgehead carboxylate-oxygen is equal to 96.6(2)° [$Cu2–O10–Cu2^{i}$] and the basal planes around the symmetry related Cu2 and $Cu2^{i}$ atoms are perfectly parallel and separated by 2.78(1) Å.

Six lithium(I) cations [Li1, Li2, Li3, $Li1^{i}$, $Li2^{ii}$, Li3 and $Li3^{i}$; symmetry code: (ii) = x, $1-y$, z] are bound to each tetranuclear $[\{Cu_2(\mu\text{-mpba})_2\}_2]^{8-}$ unit, four of them (Li1, Li2, $Li1^{i}$ and $Li2^{ii}$) being coordinated by two double carbonyl groups of two oxamate groups from two mpba ligands belonging to two tetranuclear units. These four alkaline cations exhibit a distorted square pyramidal surrounding, which is defined by one water molecule in the apical position and four oxamate-oxygens

in the basal plane. The values of τ are equal to 0.06 (Li1 and Li1^{i}) and 0.02 (Li2 and Li2^{ii}) and they are shifted from the mean basal planes by 0.46 (Li1 and Li1^{ii}) and 0.31 Å (Li2 and Li2^{ii}) towards the apical site. The two remaining lithium atoms (Li3 and Li3^{ii}) are also bonded to two tetracopper(II) units, but the coordination to the oxamate group in a monodentate form shares one oxygen atom of a carboxylate group with other lithium(I) ion. They are four-coordinate in a tetrahedral geometry with two water molecules completing the coordination sphere. Lithium(I) ions connect the tetranuclear units along the crystallographic *b* axis extending the motif to an 1D coordination polymer $\{Li_6(H_2O)_8[Cu_4(\mu\text{-mpba})_4(H_2O)_2]\}^{2-}$, in which the copper(II) ions separated along lithium bridges are distant from each other by 10.371(2) Å (Figure 2a). The resulting ladder-like double chain structure is interlinked through the $EDAP^{2+}$ cations, these counterions joining the ladders along the crystallographic *c* axis by means of hydrogen bonds involving their terminal NH_2 groups and the carboxylate oxygen atoms (Figure 2b). Since the $EDAP^{2+}$ cations in this compound show the *anti* conformation around their CH_2–CH_2 centers, the pyridyl groups are not coplanar and occupy different layers, interconnecting ladders from different crystal packing layers and guaranteeing the 3D structure.

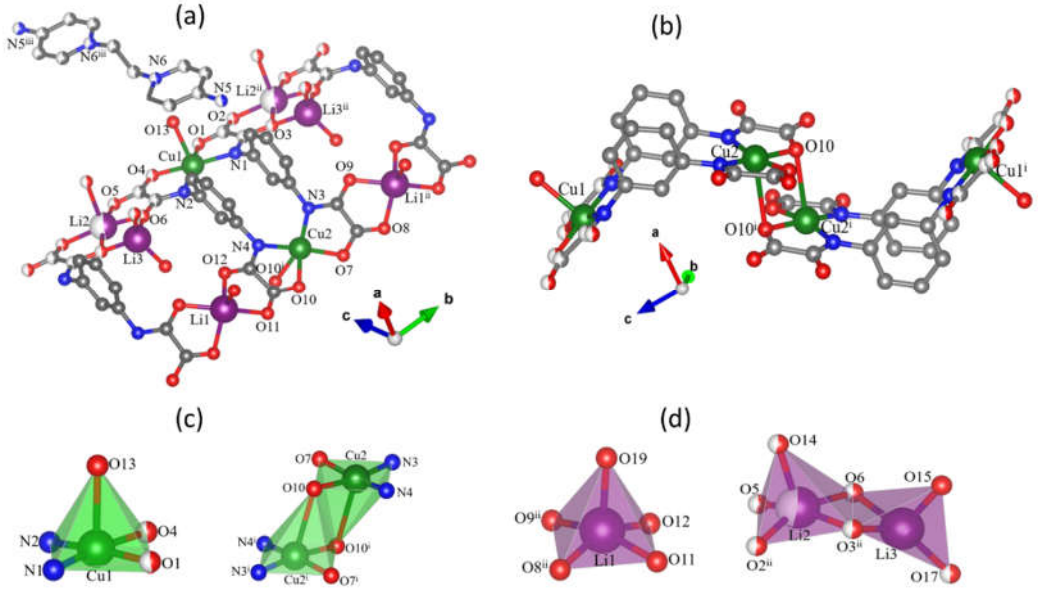

Figure 1. (**a**) Perspective view of the dicopper [3,3] metallacyclophane-type fragment of **1** with the atom labelling scheme. Carbon and hydrogen atoms are displayed as dark and light gray spheres. Atoms with half of sphere in white represent the disordered atoms. Hydrogen atoms were omitted for clarity. (**b**) The crystal structure of the centrosymmetric tetracopper(II) $[Cu_4(\mu\text{-mpba})_4(H_2O)_2]^{8-}$ fragment in **1** [symmetry code: (i) = $2-x, 1-y, 1-z$; (ii) = $x, 1-y, z$]. (**c**) Coordination polyhedra of the copper(II) and (**d**) lithium(I) ions, respectively. Atomic displacement ellipsoids of **1** can be found in the Supplementary Information, Figure S5.

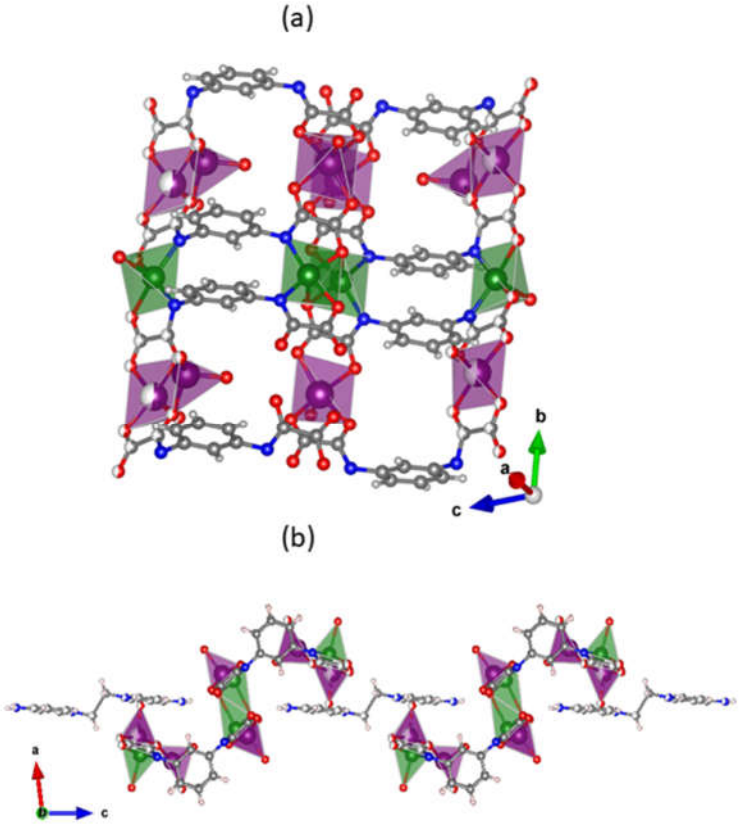

Figure 2. (**a**) Fragment of the $\{Li_6(H_2O)_8[Cu_4(\mu\text{-mpba})_4(H_2O)_2]\}^{2-}$ 1D coordination polymer growing parallel to the crystallographic *b* axis featuring the coordination polyhedra of the metal ions [color code: purple for lithium(I) and green for copper(II)]. (**b**) Crystal packing of **1** along the crystallographic *c* axis showing the $\{Li_6(H_2O)_8[Cu_4(\mu\text{-mpba})_4(H_2O)_2]\}^{2-}$ units separated by the $EDAP^{2+}$ cations which create bridges between coordination polymers via hydrogen bonds. Atomic displacement ellipsoids of **2** can be found in the Supplementary Information, Figure S6.

Compound **2** is made up of $[Cu_2(\mu\text{-mpba})_2(H_2O)_2]^{4-}$ dicopper(II) units which act as ligands towards tetraaquapotassium(I) entities, non-coordinated chloride anions and $EDAP^{2+}$ cations allowing the achievement of the electroneutrality (Figure 3a). Disordered crystallization water molecules are found filling the voids in the structure. Each crystallographically independent copper(II) ion in **2** (Cu1) is five-coordinate in a *cis*-CuN_2O_3 environment (Figure 3b), just as found for **1** and related compounds in the literature. The value of τ for this copper atom is equal to 0.01. Two oxamate groups from two mpba ligands occupy the basal plane and the apical site is filled by a water molecule. The copper(II) ion is slightly lifted from the mean basal plane, being 0.03 Å above it. The copper-copper separation within the [3,3] metallacyclophane-type unit in **2** is equal to 7.056(1) Å and the angle between the basal planes of each copper atom is 47.4(1)°. This smaller angle, compared to **1**, is most likely caused by the potassium coordination to both carboxylate groups, forming double Cu–$(\mu\text{-O})_2$–K bridges [Cu1–O1–K1 and Cu1–$O4^{i}$–K1; symmetry code (i) = $5/2 - x, y, 2 - z$] which tide the carboxylate groups and force their approximation and thus a more distorted square base at the copper atom [the carboxylate oxygen atoms in **1** are 2.754(1) Å far from each other whereas they are 2.675(1) Å in **2**]. The distortions are also observed in the phenyl rings. Since the carboxylate groups are close, the phenyl rings are farther than in **1**, with their geometric centers at 3.44 Å and their mean planes forming a dihedral angle of 9.15(1)°.

Each potassium cation in **2** is eight-coordinate with four carboxylate-oxygens and four water molecules building a distorted square antiprism geometry (Figure 3c). Like in **1,** the alkaline cation extends the structure into 1D coordination polymers of formula $\{K(H_2O)_4[Cu_2(\mu\text{-mpba})_2(H_2O)_2]\}_n^{3n-}$, differently from **1** in which the alkaline ion is coordinated by the carbonyl amide and the carboxylate

groups. The single chains in **2** exhibit a zig zag conformation using the intrinsic bend of the 1,3-substituted ligand, as pictured in Figure 4a. This pattern raises along the crystallographic *a* axis and voids filled with the two disordered crystallization water molecules (the number of crystallization water molecules was determined by TG/DTA analysis) can be found along the crystallographic *b* axis. Finally, the 1D coordination polymers are packed in the crystallographic *ac* plane and they are intercalated with layers of $EDAP^{2+}$ cations (Figure 4b).

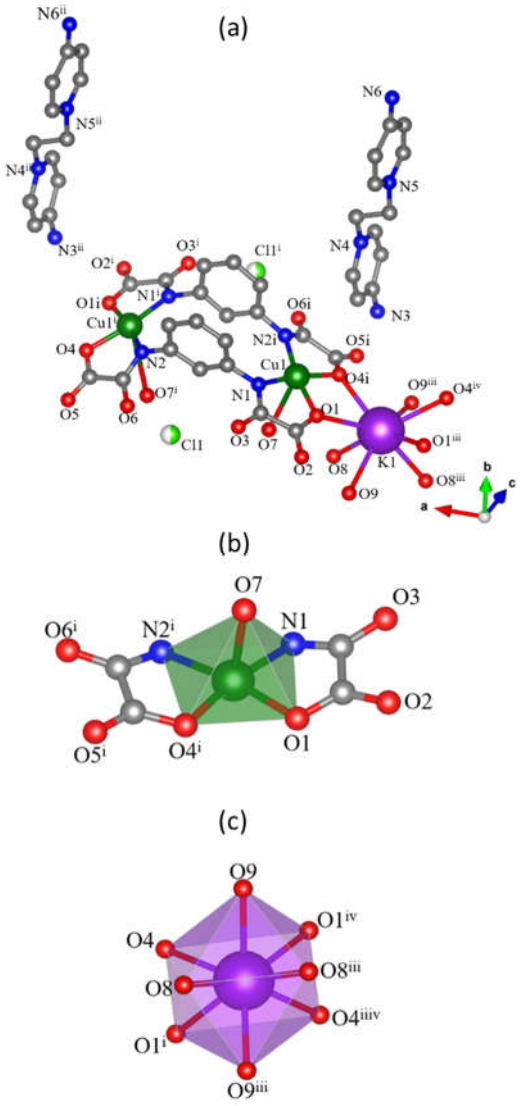

Figure 3. (**a**) Representation of a fragment of the structure of **2**. Carbon and hydrogen atoms are displayed as dark and pale gray spheres. Two chlorine atoms are present since each position is equivalent to half of the occupancy for this atom. Crystallization water molecules are hidden for the sake of clarity [symmetry code: (i) = $5/2 - x$, y, $2 - z$; (ii) = $5/2 - x$, $-1/2 - y$, $3/2 - z$; (iii) = $3/2 - x$, y, $2 - z$; (iv) = $-1 + x$, y, z]. (**b**) Coordination polyhedron of the copper atom. (**c**) Coordination polyhedron of the potassium atom.

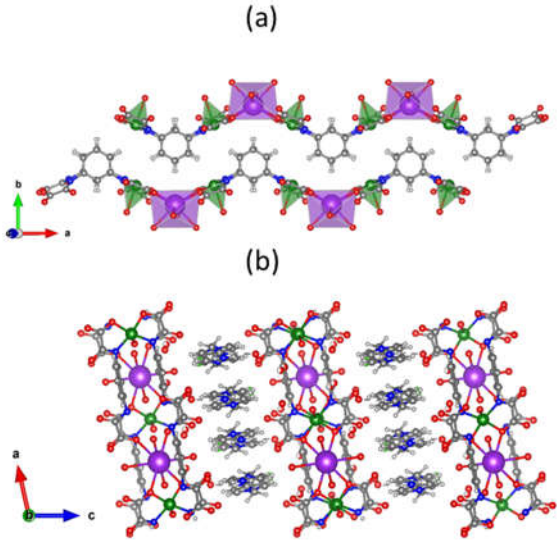

Figure 4. (**a**) View of the packing of two adjacent heterobimetallic chains along the crystallographic *a* axis in **2**. $EDAP^{2+}$ cations are omitted for clarity. (**b**) Intercalated layers of $EDAP^{2+}$ cations separating the layers of $\{K(H_2O)_4[Cu_2(\mu\text{-mpba})_2(H_2O)_2]\}_n^{3n-}$ polymers packed along the crystallographic *ab* plane. The crystallization water molecules were omitted in both figures for the sake of clarity.

3.2. Magnetic Study

Magnetic properties of **1** in the form of the $\chi_M T$ *versus* T plot [χ_M is the magnetic susceptibility per four copper(II) ions] are shown in Figure 5. $\chi_M T$ at 300 K is equal 1.59 cm^3 mol^{-1} K, a value which is consistent with the presence of four magnetically isolated spin doublets (ca. 1.58 cm^3 mol^{-1} K for $S_{Cu} = 1/2$ and $g_{Cu} = 2.05$). Upon cooling, a smooth increase of $\chi_M T$ occurs below 100 K to reach a maximum of 1.98 cm^3 mol^{-1} K at 9.0 K and exhibiting a further decrease to 1.77 cm^3 mol^{-1} K at 2.0 K. This plot is typical of an overall ferromagnetic behavior, the small decrease at very low temperatures being most likely due to very weak (intra/intermolecular) antiferromagnetic interactions and/or zero-field splitting effects. No maximum of χ_M is observed in the χ_M against T plot (see inset in Figure 5).

Having in mind the tetracopper(II) unit of **1** and aiming at evaluating the magnitude and nature of the magnetic interactions in this compound, its magnetic data were analyzed through the Hamiltonian of equation (1):

$$\boldsymbol{H} = -J(\boldsymbol{S}_{Cu1}\cdot\boldsymbol{S}_{Cu2} + \boldsymbol{S}_{Cu1^i}\cdot\boldsymbol{S}_{Cu2^i}) - j(\boldsymbol{S}_{Cu2}\cdot\boldsymbol{S}_{Cu2^i}) + g\beta H(\boldsymbol{S}_{Cu1} + \boldsymbol{S}_{Cu2} + \boldsymbol{S}_{Cu2^i} + \boldsymbol{S}_{Cu1^i}) \quad (1)$$

in which J and j are the magnetic coupling parameters between the copper(II) ions across the *meta* substituted phenyl ring of the mpba ligand and through the double out-of-plane carboxylate(oxamate)-oxygen exchange pathway, respectively. An average Landé factor ($g = g_{Cu1} = g_{Cu2}$) was assumed for the two crystallographically independent copper(II) in order to avoid any overparametrization. The deduced analytical expression is given by equation (2) [46]:

$$\chi_M T = \frac{2N\beta g^2 2}{k}\left[\frac{5e^{-\frac{A1}{kT}} + e^{-\frac{A2}{kT}} + e^{-\frac{A3}{kT}} + e^{-\frac{A4}{kT}}}{5e^{-\frac{A1}{kT}} + 3e^{-\frac{A2}{kT}} + 3e^{-\frac{A3}{kT}} + 3e^{-\frac{A4}{kT}} + 5e^{-\frac{A5}{kT}} + e^{-\frac{A6}{kT}}}\right] \quad (2)$$

$$A1 = -\frac{j}{4} - \frac{J}{2};$$

$$A2 = -\frac{j}{4} + \frac{J}{2};$$

$$A3 = \frac{j}{4} + \frac{\sqrt{J^2 + j^2}}{2};$$

$$A4 = \frac{j}{4} - \frac{\sqrt{J^2 + j^2}}{2};$$

$$A5 = \frac{j}{4} + \frac{J}{2} + \frac{\sqrt{4j^2 - 2Jj + 2J^2}}{2};$$

$$A6 = \frac{j}{4} + \frac{J}{2} - \frac{\sqrt{4j^2 - 2Jj + 2J^2}}{2};$$

in which N, β and k have their usual meanings. The best-fit parameters are: J = +10.63 cm^{-1}, j = −0.68 cm^{-1}, g = 2.05 and R = 1.4 × 10^{-5} (R is the agreement factor defined as $\Sigma[(\chi_M T)_{obs} - (\chi_M T)_{calc}]^2/\Sigma[(\chi_M T)_{obs}{}^2]$). The calculated curve (solid line in Figure 5) reproduces well the magnetic data in the whole temperature range explored.

The ferromagnetic interaction in **1** (J = +10.63 cm^{-1}) is unambiguously mediated by the double Cu1–$N_{amidate}$–$(C–C–C)_{phenyl}$–$N_{amidate}$–Cu2 exchange pathway, being once more a nice example of the efficiency of the spin polarization mechanism to transmit ferromagnetic interactions between copper(II) ions separated by *ca.* 7 Å in this type of *meta*-substituted bis-oxamate ligands [12,47–49]. The ferromagnetic coupling in this compound is explained by the spin polarization mechanism operating in the Cu–$N_{amidate}$–C_{ring}–C_{ring}–C_{ring}–N_{amide}–Cu fragment. The alternating sign of the spin density in this pathway leads to the same sign on the two copper(II) ions. In comparison with the first dicopper(II) compound containing mpba ligands reported in literature $Na_4[Cu_2(\mu\text{-mpba})_2]\cdot 10H_2O$ [12], J value for **1** is smaller than the one observed (see Table 4). This may be understood by comparing the values of the torsion angle (ϕ) involving the Cu–$N_{amidate}$ bonds and the aromatic spacers. The closer this angle is to 90° and the greater the planarity of the aromatic spacer, the stronger is the ferromagnetic coupling through this pathway. This angle in **1** vary from 71.5(3) to 85.9(9)°, a value which is smaller than those occurring in the related compound $Na_4[Cu_2(\mu\text{-mpba})_2]\cdot 10H_2O$ [ϕ in the range 72.1(3)–82.0(3)°] [12], this fact accounts for the weakening of the ferromagnetic coupling in **1**.

Concerning the value of j (−0.68 cm^{-1}), it unambiguously corresponds to the interaction between Cu1 and Cu1^{i} atoms through the double out-of-plane carboxylate(oxamate)-oxygen pathway. For such a situation, weak ferro- and antiferromagnetic couplings were reported in the literature, its sign and magnitude being dependent on subtle structural factors such as the value of the angle at the bridgehead oxygen and the apical copper-to oxygen bond length (see Table 4). Simple orbital symmetry considerations allow to understand this situation. For a copper(II) ion in a square pyramidal surrounding like Cu2 (and the symmetry related Cu2^{i}), the unpaired electron is mainly defined by a $d_{x^2-y^2}$ magnetic orbital which spreads its density only over the basal plane, a poor spin density being expected on the apical site. Then, the overlap between the parallel magnetic orbitals of Cu2 and Cu2^{i} is predicted to be very weak leading to a very weak antiferromagnetic interaction. Depending on the value of the angle at the bridgehead oxygen, accidental orthogonality of the magnetic orbitals may result and the interaction would become weakly ferromagnetic. The j value found in **1** is in the range of those reported in the literature for the double out-of-plane copper(II)-carboxylate-oxygen bridged compounds, as shown in Table 4.

Table 4. Comparison of the magnetic exchange between copper(II) ions in **1** and in other dicopper(II) *meta*-substituted phenyl(pyridyl) bis-oxamate or double out-of-plane μ-oxo(carboxylate) complexes.

Compound [a]	J [b]/cm^{-1}	j [c]/cm^{-1}	d_{axial} [d]/Å	Θ [e]/K	θ_{CuOCu} [f]/°	Reference
1	+10.6	−0.68	2.682		96.7	This work
2	+8.22			+0.27		This Work
$Na_4[Cu_2(\mu\text{-mpba})_2]\cdot 10H_2O$	+16.8	—	—		—	[12]
$[Cu_2(\mu\text{-mpba})_2(H_2O)F]$ $[Cu(L^1)]_4(PF_6)_3\cdot 5H_2O$	+17.0	—	—		—	[47]
$[Cu_2(L^2)_2(H_2O)_2][Cu(L^1)]_4(ClO_4)_4\cdot 12H_2O$	+9.0	—	—		—	[47]
$[Ni(L^3)][Cu_2(\mu\text{-mpba})_2][Ni(L^3)]_3(ClO_4)_4\cdot 6H_2O$	+4.2	—	—		—	[47]
$(Me_4N)_4[Cu_2(L^4)_2(H_2O)]_2\cdot H_2O$	+6.85	—	—		—	[48]
$(Me_4N)_2KNa[Cu(L^4)_2(H_2O)_{6.8}]\cdot 0.8H_2O$	+7.40	—	—		—	[48]
$Na_6[Cu_2(L^4)_2Cl_2(H_2O)_4]\cdot 7H_2O$	+7.90	—	—		—	[48]
$[Cu(L^5)(\mu\text{-tfa})]_2$	—	−3.30	2.630		105.7	[50]
$[Cu(H_2L^6)(\mu\text{-EtOH})]_2$	—	+2.93	2.365		102.5	[51]
$[Cu(L^7)(\mu\text{-OAc})]_2$	—	−0.37	2.399		102.2	[52]
$[Cu(phen)(\mu\text{-}L^8)]_2$	—	+1.80	2.340		103.0	[53]
$[Cu(bpy)\text{-}(\mu\text{-}L^9)]_2$	—	+1.50	2.369		104.9	[53]
$[Cu(phen)(\mu\text{-}L^{10})]_2\cdot H_2L^4$	—	+3.20	2.320		101.9	[54]
$[Cu(im)(\mu\text{-}L^{11})]_2\cdot 2H_2O$	—	+0.58	2.571		102.5	[55]
$[Cu(L^{12})(\mu\text{-OAc})]_2$	—	−0.50	2.490		95.3	[56]
$[Cu(L^{13})(\mu\text{-OAc})]_2\cdot 2H_2O$	—	−1.51	2.577		96.1	[57]
$[Cu(L^{14})(\mu\text{-OAc})]_2\cdot 2H_2O$	—	−1.84	2.665		96.3	[57]
$[Cu(L^{15})(\mu\text{-OAc})]_2$	—	+2.85	2.440		98.1	[58]
$[Cu(L^{16})(\mu\text{-}HL^{11})]_2$	—	−2.03	2.299		103.3	[59]
$Na_2(C_{12}H_{12}N_2)[Cu(L^{17})]_2\cdot 4H_2O$	—	−0.80	2.788		95.4	[38]
$[Cu(L^{18})(\mu\text{-OAc})]_2$	—	−0.56	2.501		98.7	[60]
$[Cu(phen)(\mu\text{-}L^{19})]_2$	—	+3.30	2.332		104.6	[61]
$[Cu(L^{20})(\mu\text{-OAc})]_2\cdot H_2O\cdot EtOH$	—	+0.63	2.650		102.6	[62]
$(EDAP)_2[Cu(L^{17})]_2\cdot 4H_2O$	—	−1.63	2.591		96.1	[26]
$Na_2(EDAP)[Cu(L^{17})]_2\cdot 6H_2O$	—	−2.29	2.616		93.7	[26]
$K_2(EDAP)[Cu(L^{17})]_2\cdot 5H_2O$	—	−1.65	2.911		94.1	[26]

[a] Ligand abbreviations: L^1 = *N*,*N*,*N*′,*N*″, *N*″-pentamethyldiethylenetriamine; H_4L^2 = 2, 4, 6-trimethyl-*N*,*N*′-1, 3-phenylenebis(oxamic acid); L^3 = 1,4,8,11-tetraazacyclotetradecane; H_4L^4 = *N*,*N*′-2 , 6-pyridinebis(oxamic acid); HL^5 = pyridine-2-carbaldehyde thiosemicarbazone; tfa = trifluoroacetate; H_4L^6 = *N*,*N*′-2,2′-ethylenediphenylenebis(oxamic acid); L^7 = 2-(((2-(dimethylamino)ethyl)imino)methyl)-phenolate, OAc = acetate; H_2L^8 = (2*S*,3*R*)-oxirane-2, 3-dicarboxylic acid; phen = 1,10-phenantroline; bpy = 2,2′-bipyridine; L^9 = thiodiacetate; L^{10} = phenylacetate, im = imidazole; L^{11} = 7-amino-4-methyl-5-aza-3-hepten-2-one; L^{12} = *N*-methyl-*N*′-(5-nitrosalicy1idene)-1, 3-propanediamine; L^{13} = *N*-methyl-*N*′-(5-bromosalicy1idene)-1, 3-propanediamine; HL^{14} = 4-[(3-aminopentylimino)-methyl]-benzene-1,3-diol; L^{15} = N3-benzoylpyridine-2-carboxamidrazone; H_2L^{16} = phtalic acid; $C_{12}H_{12}N_2$ = 6,7-dihydrodipyrido(1,2-*a*:2′,1′-*c*)pyrazinium; H_4L^{17} = *N*,*N*′-1,2-phenylenebis(oxamic acid); HL^{18} = 4-(2-ethylamino-ethylimino)-pentan-2-one; L^{19} = oxydiacetate dianion; HL^{20} = *N*-(l,l-dimethyl-2-hydroxyethyl)salicylaldimine. [b] Magnetic coupling between the copper(II) ions through the 1, 3-phenyl/pyridyl oxamidate pathway. [c] Magnetic coupling between the copper(II) ions across the double out-of-plane monoatomic carboxylate bridge. [d] Copper-copper separation through the double out-of-plane monoatomic carboxylate bridge. [e] Curie-Weiss term. [f] Cu–O–Cu angle involving the carboxylate bridge.

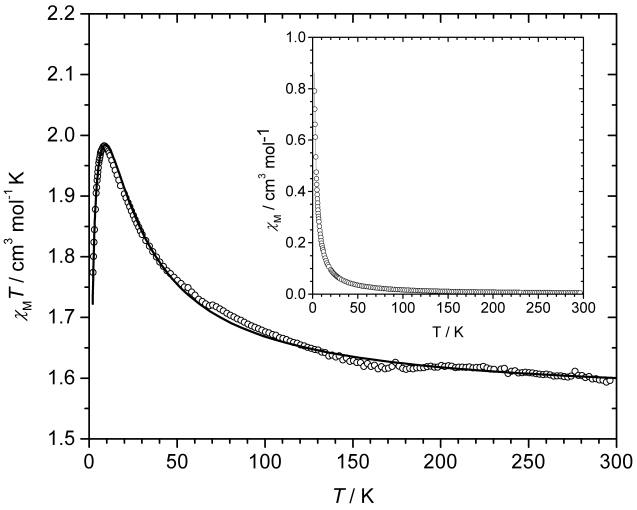

Figure 5. Temperature dependence of the $\chi_M T$ product for **1**: (○) experimental; (—) best-fit curve through Equation (3) (see text). Inset: χ_M versus T plot.

The magnetic properties of **2** in the form of $\chi_M T$ against T plot [$\chi_M T$ is the magnetic susceptibility per two copper(II) ions] are shown in Figure 6. At room temperature, $\chi_M T$ is equal to 0.81 cm^3 mol^{-1} K, a value which is as expected for two magnetically non-interacting spin doublets. Upon cooling, this value remains practically constant until 150 K and it further increases continuously to reach 1.24 cm^3 mol^{-1} K at 2.0 K. This plot is typical of an overall ferromagnetic behavior.

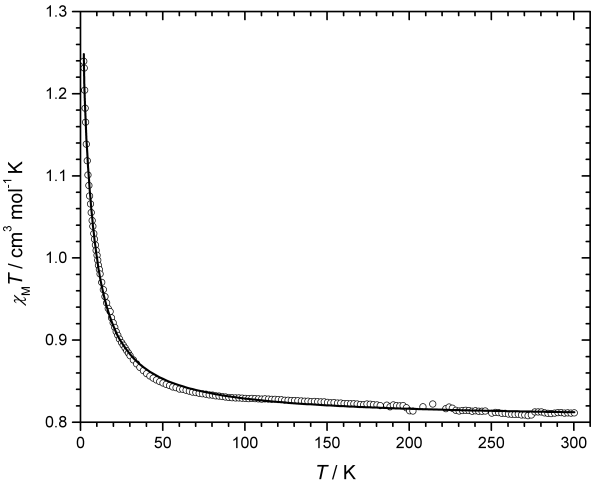

Figure 6. Temperature dependence of the $\chi_M T$ product for **2**: (○) experimental; (—) best-fit curve through Equation (1) (see text).

The magnetic data of **2** were analyzed through the spin Hamiltonian for an isolated pair of isotropic metal ions [Equation (3)]

$$\boldsymbol{H} = -JS_1 \cdot S_2 + g\beta H(S_1 + S_2) \quad (3)$$

in which J is the magnetic coupling parameter, $S_1 = S_2 = 1/2$ and g is the isotropic Landé factor of the copper(II) ions. In this case, the equation derived from the Hamiltonian is the Bleaney-Bowers expression (equation (4)) [63]:

$$\chi_M = \left[\frac{2N^2g^2}{k(T-\theta)}\right][3+\exp(-J/kT)]^{-1} \quad (4)$$

A Curie-Weiss term (θ) was introduced in Equation (4) to take into account the possible intermolecular interactions. Best-fit parameters are: J = +8.22 cm^{-1}, g = 2.07 and θ = +0.27 K with $R = 2.15 \times 10^{-4}$. The magnetic coupling within the dicopper(II) [3,3] metallacyclophane fragment in **2** (J = +8.22 cm^{-1}) is of identical nature with that in **1** (J = +7.14 cm^{-1}), although it is somewhat smaller. The same spin polarization mechanism involved in **1** occurs in **2**, but the different values of J found for them can be understood by a comparison of some structural parameters within their dicopper(II) fragments. The dihedral angle between the Cu–$N_{amidate}$ bond and the aromatic spacer in **2** [47.4(1)°] is smaller than the corresponding one in **1** [59.2(2)°], indicating that the spin polarization mechanism to mediate ferromagnetic interactions between copper(II) ions through this pathway would be more efficient in **1**. This subtle structural difference accounts for the somewhat weakening of the ferromagnetic coupling when going from **1** to **2** [12,48].

4. Conclusions

This work shows that the use of templating organic counterions such as $EDAP^{2+}$ and coordinated alkaline cations may play a relevant structural role in the assembling of 1D coordination polymers with ladder-like double chain or zig zag chain structures depending on the nature of the univalent alkaline cation. Remarkably, the use of the lithium(I) leads to the tetranuclear copper(II)-oxamate unit in compound **1**, in which two dicopper(II) [3,3] metallacyclophane-type entities are assembled throughout double out-of-plane interactions. As far as we know, it is the first time that such a tetracopper(II) unit with the mpba ligand is described. Although compound **1** presents a satisfactory R_{int} indicator, due to intrinsic crystals quality and twinning, the refinement indicators are out of routine of the X-ray crystallography for small molecules, but its crystal structure is corroborated by chemical analysis and it matches the theoretical models based on it which were proposed to treat the magnetic properties. Compound **2** is obtained when the lithium(I) cations are replaced by the potassium(I) ones where this assembling does not occur and the dicopper(II) [3,3] metallacyclophane units are interconnected through the alkaline cations. Moderate ferromagnetic couplings between the copper(II) ions separated by more than *ca.* 7.0 Å in the metallamacrocycles of the [3,3] metallacyclophane-type of **1** and **2** are observed, the spin polarization mechanism being responsible for them.

Supplementary Materials: The following are available online at http://www.mdpi.com/2312-7481/4/3/38/s1, Figure S1: TG curve of **1**, Figure S2: TG curve of **2**, Figure S3: Experimental and Simulated X-ray powder diffraction patterns for **1**, Figure S4: Experimental and simulated X-ray powder diffraction patterns for **2**, Figure S5: Perspective view of the dicopper [3,3] metallacyclophane-type fragment of **1** with atomic displacement ellipsoids at 50% of probability. Circles represents isotropically treated disordered atoms. Color code: carbon (grey), nitrogen (sky blue), lithium (purple) and copper (green), Figure S6: Representation of a fragment of the structure of **2** with atomic displacement ellipsoids at 50% of probability. Circles represents isotropically treated disordered atoms. Color code: carbon (grey), nitrogen (sky blue), lithium (purple) and copper (green) [Symmetry code: (i) = $5/2 - x$, y, $2 - z$].

Author Contributions: T.T.d.C. performed the synthesis of compounds and also the IR, elemental analyses and atomic absorption measurements. W.X.C.O. carried out X-ray diffraction measurements. E.F.P. took the magnetic measurements and calculated the best-fit curves. M.J. and F.L. interpreted all results and contributed to the revision of this manuscript. C.L.M.P. designed the synthesis, supervised all the experiments, interpreted all results and was the responsible scientist for Funding Acquisition. All authors contributed to the writing of the manuscript.

Funding: This work was supported by Conselho Nacional de Desenvolvimento Científico e Tecnológico (CNPq) (Projects 405199/2016-3 and 308836/2015-4), Fundação de Amparo à Pesquisa do Estado de Minas Gerais (FAPEMIG) (Project PPM-00508-16), Coordenação de Aperfeiçoamento de Pessoal de Nível Superior (CAPES) and Ministerio Español the Economía y Competitividad (Projects CTQ2016-75068P and Unidad de Excelencia María de Maetzu MDM2015-0538).

Acknowledgments: Authors are grateful to Labri (Laboratório de Cristalografia), from Universidade Federal de Minas Gerais, and R.M. Lago and his Ph.D. student P.S. Pinto for thermogravimetric analyses.

Conflicts of Interest: The authors declare no conflict of interest.

References

1. Ferrando-Soria, J.; Vallejo, J.; Castellano, M.; Martínez-Lillo, J.; Pardo, E.; Cano, J.; Castro, I.; Lloret, F.; Ruiz-García, R.; Julve, M. Molecular magnetism, quo vadis? A historical perspective from a coordination chemist viewpoint. *Coord. Chem. Rev.* **2017**, *339*, 17–103. [CrossRef]
2. Stadler, R. Electrons in Molecules. From Basic Principles to Molecular Electronics. By Jean-Pierre Launay and Michel Verdaguer. *Angew. Chem. Int. Ed.* **2014**, *53*, 6307. [CrossRef]
3. Ruiz, R.; Lloret, F.; Julve, M.; Faus, J.; Carmen Muñoz, M.; Solans, X. Structure and magnetic properties of a linear oximato-bridged tetranuclear copper(II) complex. *Inorg. Chim. Acta* **1998**, *268*, 263–269. [CrossRef]
4. Teipel, S.; Griesar, K.; Haase, W.; Krebs, B.A. A New-Type of μ_4-Oxo-Bridged Copper Tetramer-Synthesis, X-Ray Molecular-Structure, Magnetism and Spectral Properties of (μ_4-Oxo)Tetrakis(μ-Bromo)bis(μ-2,6-bis(Morpholinomethyl)-4-Methylphenolato)Tetracopper(II) and (μ_4-Oxo)Tetrakis(μ-Benzoato)bis(μ-2,6-bis(Morpholinomethyl)-4-Methylphenolato)Tetracopper(II). *Inorg. Chem.* **1994**, *33*, 456–464.
5. Colacio, E.; Ghazi, M.; Kivekäs, R.; Moreno, J.M. Helical-Chain Copper(II) Complexes and a Cyclic Tetranuclear Copper(II) Complex with Single Syn−Anti Carboxylate Bridges and Ferromagnetic Exchange Interactions. *Inorg. Chem.* **2000**, *39*, 2882–2890. [CrossRef] [PubMed]
6. Song, Y.; Massera, C.; Roubeau, O.; Gamez, P.; Lanfredi, A.M.M.; Reedijk, J. An Unusual Open Cubane Structure in a $\mu_{1,1}$-Azido- and Alkoxo-Bridged Tetranuclear Copper(II) Complex, $[Cu_4L_2(\mu_{1,1}\text{-}N_3)_2]\cdot 5H_2O$ (H_3L = *N*,*N*′-(2-Hydroxylpropane-1,3-diyl)bis-salicylideneimine). *Inorg. Chem.* **2004**, *43*, 6842–6847. [CrossRef] [PubMed]
7. Kruger, P.E.; Moubaraki, B.; Fallon, G.D.; Murray, K.S. Tetranuclear copper(II) complexes incorporating short and long metal-metal separations: Synthesis, structure and magnetism. *J. Chem. Soc. Dalton Trans.* **2000**, *5*, 713–718. [CrossRef]
8. Murugesu, M.; Clérac, R.; Pilawa, B.; Mandel, A.; Anson, C.E.; Powell, A.K. Ferromagnetic interactions mediated by syn–anti carboxylate bridging in tetranuclear copper(II) compounds. *Inorg. Chim. Acta* **2002**, *337*, 328–336. [CrossRef]
9. Santana, M.D.; García, G.; Julve, M.; Lloret, F.; Pérez, J.; Liu, M.; Sanz, F.; Cano, J.; López, G. Oxamidate-Bridged Dinuclear Five-Coordinate Nickel(II) Complexes: A Magneto−Structural Study. *Inorg. Chem.* **2004**, *43*, 2132–2140. [CrossRef] [PubMed]
10. Pardo, E.; Faus, J.; Julve, M.; Lloret, F.; Muñoz, M.C.; Cano, J.; Ottenwaelder, X.; Journaux, Y.; Carrasco, R.; Blay, G.; et al. Long-Range Magnetic Coupling through Extended π-Conjugated Aromatic Bridges in Dinuclear Copper(II) Metallacyclophanes. *J. Am. Chem. Soc.* **2003**, *125*, 10770–10771. [CrossRef] [PubMed]
11. Chiari, B.; Helms, J.H.; Piovesana, O.; Tarantelli, T.; Zanazzi, P.F. Exchange interaction in multinuclear transition-metal complexes. 9. Magnetostructural correlations in one-atom acetato-bridged copper(II) dimers. *Inorg. Chem.* **1986**, *25*, 2408–2413. [CrossRef]
12. Fernández, I.; Ruiz, R.; Faus, J.; Julve, M.; Lloret, F.; Cano, J.; Ottenwaelder, X.; Journaux, Y.; Muñoz, M.C. Ferromagnetic Coupling through Spin Polarization in a Dinuclear Copper(II) Metallacyclophane. *Angew. Chem. Int. Ed.* **2001**, *40*, 3039–3042. [CrossRef]
13. Pardo, E.; Morales-Osorio, I.; Julve, M.; Lloret, F.; Cano, J.; Ruiz-García, R.; Pasán, J.; Ruiz-Pérez, C.; Ottenwaelder, X.; Journaux, Y. Magnetic Anisotropy of a High-Spin Octanuclear Nickel(II) Complex with a meso-Helicate Core. *Inorg. Chem.* **2004**, *43*, 7594–7596. [CrossRef] [PubMed]
14. Dul, M.C.; Pardo, E.; Lescouëzec, R.; Journaux, Y.; Ferrando-Soria, J.; Ruiz-García, R.; Cano, J.; Julve, M.; Lloret, F.; Cangussu, D.; et al. Supramolecular coordination chemistry of aromatic polyoxalamide ligands: A metallosupramolecular approach toward functional magnetic materials. *Coord. Chem. Rev.* **2010**, *254*, 2281–2296. [CrossRef]
15. Simões, T.R.G.; do Pim, W.D.; Silva, I.F.; Oliveira, W.X.C.; Pinheiro, C.B.; Pereira, C.L.M.; Lloret, F.; Julve, M.; Stumpf, H.O. Solvent-driven dimensionality control in molecular systems containing Cu^{II}, 2,2′-bipyridine and an oxamato-based ligand. *CrystEngComm* **2013**, *15*, 10165–10170. [CrossRef]

16. Qu, X.; Song, X.; Li, W.; Xu, Y.; Li, L.; Liao, D.; Jiang, Z. Structural and Magnetic Properties of Two Copper(II) Complexes Based on Dinuclear Copper(II) Metallacyclophane. *Eur. J. Inorg. Chem.* **2008**, *8*, 1287–1292. [CrossRef]
17. Pereira, C.L.M.; Pedroso, E.F.; Stumpf, H.O.; Novak, M.A.; Ricard, L.; Ruiz-García, R.; Rivière, E.; Journaux, Y. A $Cu^{II}Co^{II}$ Metallacyclophane-Based Metamagnet with a Corrugated Brick-Wall Sheet Architecture. *Angew. Chem. Int. Ed.* **2004**, *43*, 956–958. [CrossRef] [PubMed]
18. Cangussu, D.; Pardo, E.; Dul, M.C.; Lescouëzec, R.; Herson, P.; Journaux, Y.; Pedroso, E.F.; Pereira, C.L.M.; Stumpf, H.O.; Carmen Muñoz, M.; et al. Rational design of a new class of heterobimetallic molecule-based magnets: Synthesis, crystal structures, and magnetic properties of oxamato-bridged $M_3'M_2$ (M' = Li^{I} and Mn^{II}; M = Ni^{II} and Co^{II}) open-frameworks with a three-dimensional honeycomb architecture. *Inorg. Chim. Acta* **2008**, *361*, 3394–3402.
19. Lisnard, L.; Chamoreau, L.-M.; Li, Y.; Journaux, Y. Solvothermal Synthesis of Oxamate-Based Helicate: Temperature Dependence of the Hydrogen Bond Structuring in the Solid. *Cryst. Growth Des.* **2012**, *12*, 4955–4962. [CrossRef]
20. Pardo, E.; Burguete, P.; Ruiz-Garcia, R.; Julve, M.; Beltran, D.; Journaux, Y.; Amoros, P.; Lloret, F. Ordered mesoporous silicas as host for the incorporation and aggregation of octanuclear nickel(II) single-molecule magnets: A bottom-up approach to new magnetic nanocomposite materials. *J. Mater. Chem.* **2006**, *16*, 2702–2714. [CrossRef]
21. Pardo, E.; Bernot, K.; Lloret, F.; Julve, M.; Ruiz-García, R.; Pasán, J.; Ruiz-Pérez, C.; Cangussu, D.; Costa, V.; Lescouëzec, R.; et al. Solid-State Anion–Guest Encapsulation by Metallosupramolecular Capsules Made from Two Tetranuclear Copper(II) Complexes. *Eur. J. Inorg. Chem.* **2007**, *29*, 4569–4573. [CrossRef]
22. Ferrando-Soria, J.; Ruiz-García, R.; Cano, J.; Stiriba, S.-E.; Vallejo, J.; Castro, I.; Julve, M.; Lloret, F.; Amorós, P.; Pasán, J.; et al. Reversible Solvatomagnetic Switching in a Spongelike Manganese(II)–Copper(II) 3D Open Framework with a Pillared Square/Octagonal Layer Architecture. *Chem. Eur. J.* **2012**, *18*, 1608–1617. [CrossRef] [PubMed]
23. Ferrando-Soria, J.; Serra-Crespo, P.; de Lange, M.; Gascon, J.; Kapteijn, F.; Julve, M.; Cano, J.; Lloret, F.; Pasán, J.; Ruiz-Pérez, C.; et al. Selective Gas and Vapor Sorption and Magnetic Sensing by an Isoreticular Mixed-Metal–Organic Framework. *J. Am. Chem. Soc.* **2012**, *134*, 15301–15304. [CrossRef] [PubMed]
24. Grancha, T.; Acosta, A.; Cano, J.; Ferrando-Soria, J.; Seoane, B.; Gascon, J.; Pasán, J.; Armentano, D.; Pardo, E. Cation Exchange in Dynamic 3D Porous Magnets: Improvement of the Physical Properties. *Inorg. Chem.* **2015**, *54*, 10834–10840. [CrossRef] [PubMed]
25. Oliveira, W.X.C.; Ribeiro, M.A.; Pinheiro, C.B.; da Costa, M.M.; Fontes, A.P.S.; Nunes, W.C.; Cangussu, D.; Julve, M.; Stumpf, H.O.; Pereira, C.L.M. Palladium(II)–Copper(II) Assembling with Bis(2-pyridylcarbonyl)amidate and Bis(oxamate) Type Ligands. *Cryst. Growth Des.* **2015**, *15*, 1325–1335. [CrossRef]
26. Da Cunha, T.T.; Oliveira, W.X.C.; Pinheiro, C.B.; Pedroso, E.F.; Nunes, W.C.; Pereira, C.L.M. Alkaline Ion-Modulated Solid-State Supramolecular Organization in Mixed Organic/Metallorganic Compounds Based on 1,1′-Ethylenebis(4-aminopyridinium) Cations and Bis(oxamate)cuprate(II) Anions. *Cryst. Growth Des.* **2016**, *16*, 900–907. [CrossRef]
27. Abdulmalic, M.A.; Aliabadi, A.; Petr, A.; Kataev, V.; Ruffer, T. The formation of overlooked compounds in the reaction of methyl amine with the diethyl ester of o-phenylenebis(oxamic acid) in MeOH. *Dalton Trans.* **2013**, *42*, 1798–1809. [CrossRef] [PubMed]
28. Barroso, S.; Blay, G.; Fernández, I.; Pedro, J.R.; Ruiz-García, R.; Pardo, E.; Lloret, F.; Muñoz, M.C. Chemistry and reactivity of mononuclear manganese oxamate complexes: Oxidative carbon–carbon bond cleavage of vic-diols by dioxygen and aldehydes catalyzed by a trans-dipyridine manganese(III) complex with a tetradentate o-phenylenedioxamate ligand. *J. Mol. Catal. A Chem.* **2006**, *243*, 214–220. [CrossRef]
29. Oliveira, W.X.C.; Ribeiro, M.A.; Pinheiro, C.B.; Nunes, W.C.; Julve, M.; Journaux, Y.; Stumpf, H.O.; Pereira, C.L.M. Magneto-Structural Study of an Oxamato-Bridged $Pd^{II}Co^{II}$ Chain: X-ray Crystallographic Evidence of a Single-Crystal-to-Single-Crystal Phase Transition. *Eur. J. Inorg. Chem.* **2012**, *34*, 5685–5693. [CrossRef]

30. Pardo, E.; Lloret, F.; Carrasco, R.; Muñoz, M.C.; Temporal-Sánchez, T.; Ruiz-García, R. Chemistry and reactivity of dinuclear iron oxamate complexes: Alkane oxidation with hydrogen peroxide catalysed by an oxo-bridged diiron(III) complex with amide and carboxylate ligation. *Inorg. Chim. Acta* **2004**, *357*, 2713–2720. [CrossRef]
31. CrysAlisPRO. Rigaku Oxford Diffraction: Yarnton, Oxfordshire, England, 2018. Available online: https://www.rigaku.com/en/products/smc/crysalis (accessed on 2 May 2018).
32. Sheldrick, G.M. XPREP. Bruker-AXS, Madison, Wisconsin, USA. Available online: https://www.bruker.com/products/x-ray-diffraction-and-elemental-analysis/single-crystal-x-ray-diffraction/sc-xrd-software/learn-more.html (accessed on 2 May 2018).
33. Altomare, A.; Cascarano, G.; Giacovazzo, C.; Guagliardi, A.; Burla, M.C.; Polidori, G.; Camalli, M. SIR92-a program for automatic solution of crystal structures by direct methods. *J. Appl. Crystallogr.* **1994**, *27*, 435. [CrossRef]
34. Sheldrick, G.M. Crystal structure refinement with SHELXL *Acta Crystallogr. Sect. C* **2015**, *71*, 3–8.
35. Farrugia, L. WinGX and ORTEP for Windows: an update. *J. Appl. Crystallogr.* **2012**, *45*, 849–854. [CrossRef]
36. Bain, G.A.; Berry, J.F. Diamagnetic Corrections and Pascal's Constants. *J. Chem. Educ.* **2008**, *85*, 532. [CrossRef]
37. Addison, A.W.; Rao, T.N.; Reedijk, J.; van Rijn, J.; Verschoor, G.C. Synthesis, structure, and spectroscopic properties of copper(II) compounds containing nitrogen-sulphur donor ligands; the crystal and molecular structure of aqua[1,7-bis(N-methylbenzimidazol-2′-yl)-2,6-dithiaheptane]copper(II) perchlorate. *J. Chem. Soc. Dalton Trans.* **1984**, *7*, 1349–1356. [CrossRef]
38. Unamuno, I.; Gutiérrez-Zorrilla, J.M.; Luque, A.; Román, P.; Lezama, L.; Calvo, R.; Rojo, T. Ion-Pair Charge-Transfer Complexes Based on (o-Phenylenebis(oxamato))cuprate(II) and Cyclic Diquaternary Cations of 1,10-Phenanthroline and 2,2′-Bipyridine: Synthesis, Crystal Structure, and Physical Properties. *Inorg. Chem.* **1998**, *37*, 6452–6460. [CrossRef] [PubMed]
39. Reis, N.V.; Barros, W.P.; Oliveira, W.X.C.; Pereira, C.L.M.; Rocha, W.R.; Pinheiro, C.P.; Lloret, F.; Julve, M.; Stumpf, H.O. Crystal Structure and Magnetic Properties of an Oxamato-Bridged Heterobimetallic Tetranuclear $[Ni^{II}Cu^{II}]_2$ Complex of the Rack Type. *Eur. J. Inorg. Chem.* **2018**, *3–4*, 477–484. [CrossRef]
40. Oliveira, W.X.C.; Pinheiro, C.B.; da Costa, M.M.; Fontes, A.P.S.; Nunes, W.C.; Lloret, F.; Julve, M.; Pereira, C.L.M. Crystal Engineering Applied to Modulate the Structure and Magnetic Properties of Oxamate Complexes Containing the $[Cu(bpca)]^+$ Cation. *Cryst. Growth Des.* **2016**, *16*, 4094–4107. [CrossRef]
41. Pardo, E.; Bernot, K.; Julve, M.; Lloret, F.; Cano, J.; Ruiz-García, R.; Delgado, F.S.; Ruiz-Pérez, C.; Ottenwaelder, X.; Journaux, Y. Spin control in ladderlike hexanuclear copper(ii) complexes with metallacyclophane cores. *Inorg. Chem.* **2004**, *43*, 2768–2770. [CrossRef] [PubMed]
42. Pardo, E.; Cangussu, D.; Lescouëzec, R.; Journaux, Y.; Pasán, J.; Delgado, F.S.; Ruiz-Pérez, C.; Ruiz-García, R.; Cano, J.; Julve, M.; et al. Molecular-Programmed Self-Assembly of Homo- and Heterometallic Tetranuclear Coordination Compounds: Synthesis, Crystal Structures, and Magnetic Properties of Rack-Type $Cu^{II}_2M^{II}_2$ Complexes (M = Cu and Ni) with Tetranucleating Phenylenedioxamato Bridging Ligands. *Inorg. Chem.* **2009**, *48*, 4661–4673. [PubMed]
43. Ferrando-Soria, J.; Khajavi, H.; Serra-Crespo, P.; Gascon, J.; Kapteijn, F.; Julve, M.; Lloret, F.; Pasán, J.; Ruiz-Pérez, C.; Journaux, Y.; et al. Highly selective chemical sensing in a luminescent nanoporous magnet. *Adv. Mater.* **2012**, *24*, 5625–5629. [CrossRef] [PubMed]
44. Do Nascimento, G.M.; do Pim, W.D.; Reis, D.O.; Simões, T.R.G.; Pradie, N.A.; Stumpf, H.O. Characterization of compounds derived from copper-oxamate and imidazolium by X-ray absorption and vibrational spectroscopies. *Spectrochim. Acta A* **2015**, *142*, 303–310. [CrossRef] [PubMed]
45. Grancha, T.; Tourbillon, C.; Ferrando-Soria, J.; Julve, M.; Lloret, F.; Pasán, J.; Ruiz-Pérez, C.; Fabelo, O.; Pardo, E. Self-assembly of a chiral three-dimensional manganese(II)–copper(II) coordination polymer with a double helical architecture. *CrystEngComm* **2013**, *15*, 9312–9315. [CrossRef]
46. Zhang, Z.F.; Ma, Z.Y.; Wang, D.M.; Xie, C.Z. A New Linear Tetranuclear Copper(II) Complex: Synthesis, Structural Characterization, and Magnetic Behavior. *Synth. React. Inorg. Met.-Org. Nano-Met. Chem.* **2011**, *41*, 763–767. [CrossRef]

47. Pardo, E.; Ruiz-García, R.; Lloret, F.; Julve, M.; Cano, J.; Pasán, J.; Ruiz-Pérez, C.; Filali, Y.; Chamoreau, L.-M.; Journaux, Y. Molecular-Programmed Self-Assembly of Homo- and Heterometallic Penta- and Hexanuclear Coordination Compounds: Synthesis, Crystal Structures, and Magnetic Properties of Ladder-Type $Cu^{II}_2M^{II}_x$ (M = Cu, Ni; x = 3, 4) Oxamato Complexes with Cu^{II}_2 Metallacyclophane Cores. *Inorg. Chem.* **2007**, *46*, 4504–4514. [PubMed]
48. Fernandes, T.S.; Vilela, R.S.; Valdo, A.K.; Martins, F.T.; García-España, E.; Inclán, M.; Cano, J.; Lloret, F.; Julve, M.; Stumpf, H.O.; et al. Dicopper(II) Metallacyclophanes with *N*,*N*′-2,6-Pyridinebis(oxamate): Solution Study, Synthesis, Crystal Structures, and Magnetic Properties. *Inorg. Chem.* **2016**, *5*, 2390–2401. [CrossRef] [PubMed]
49. Pardo, E.; Carrasco, R.; Ruiz-García, R.; Julve, M.; Lloret, F.; Muñoz, M.C.; Journaux, Y.; Ruiz, E.; Cano, J. Structure and Magnetism of Dinuclear Copper(II) Metallacyclophanes with Oligoacenebis(oxamate) Bridging Ligands: Theoretical Predictions on Wirelike Magnetic Coupling. *J. Am. Chem. Soc.* **2008**, *130*, 576–585. [CrossRef] [PubMed]
50. Gómez-Saiz, P.; Gil-García, R.; Maestro, M.A.; Pizarro, J.L.; Arriortua, M.I.; Lezama, L.; Rojo, T.; González-Álvarez, M.; Borrás, J.; García-Tojal, J. Structure, magnetic properties and nuclease activity of pyridine-2-carbaldehyde thiosemicarbazonecopper(II) complexes. *J. Inorg. Biochem.* **2008**, *102*, 1910–1920.
51. Do Pim, W.D.; Oliveira, W.X.C.; Ribeiro, M.A.; de Faria, E.N.; Teixeira, I.F.; Stumpf, H.O.; Lago, R.M.; Pereira, C.L.M.; Pinheiro, C.B.; Figueiredo-Júnior, J.C.D.; et al. A pH-triggered bistable copper(II) metallacycle as a reversible emulsion switch for biphasic processes. *Chem. Commun.* **2013**, *49*, 10778–10780. [CrossRef] [PubMed]
52. Bhardwaj, V.K.; Aliaga-Alcalde, N.; Corbella, M.; Hundal, G. Synthesis, crystal structure, spectral and magnetic studies and catecholase activity of copper(II) complexes with di- and tri-podal ligands. *Inorg. Chim. Acta* **2010**, *363*, 97–106. [CrossRef]
53. Fang, S.M.; Sañudo, E.C.; Hu, M.; Zhang, Q.; Zhou, L.M.; Liu, C.S. Copper(II) Complexes with cis-Epoxysuccinate Ligand: Syntheses, Crystal Structures, and Magnetic Properties. *Aust. J. Chem.* **2011**, *64*, 217–226. [CrossRef]
54. Baggio, R.; Garland, M.T.; Manzur, J.; Peña, O.; Perec, M.; Spodine, E.; Vega, A. A dinuclear copper(II) complex involving monoatomic O-carboxylate bridging and Cu–S(thioether) bonds: $[Cu(tda)(phen)]_2 \cdot H_2tda$ (tda = thiodiacetate, phen = phenanthroline). *Inorg. Chim. Acta* **1999**, *286*, 74–79. [CrossRef]
55. Zhu, H.L.; Xu, W.; Lin, J.L.; Zhang, C.; Zheng, Y.-Q. Syntheses, crystal structures, and magnetism of two phenylacetate imidazolate copper(II) complexes. *J. Coord. Chem.* **2012**, *65*, 3983–3997. [CrossRef]
56. Costes, J.P.; Dahan, F.; Laurent, J.P. A further example of a dinuclear copper(II) complex involving monoatomic acetate bridges. Synthesis, crystal structure, and spectroscopic and magnetic properties of bis(μ-acetato)bis(7-amino-4-methyl-5-aza-3-hepten-2-onato(1-))dicopper(II). *Inorg. Chem.* **1985**, *24*, 1018–1022. [CrossRef]
57. Chiari, B.; Helms, J.H.; Piovesana, O.; Tarantelli, T.; Zanazzi, P.F. Exchange interaction in multinuclear transition-metal complexes. 8. Structural and magnetic studies on bis(acetato)bis(*N*-methyl-*N*′-(5-methoxysalicylidene) -1,3-propanediaminato)dicopper dihydrate, a novel "structural" ladderlike compound with "magnetic" alternating-chain behavior. *Inorg. Chem.* **1986**, *25*, 870–874.
58. Mukherjee, P.; Sengupta, O.; Drew, M.G.B.; Ghosh, A. Anion directed template synthesis of Cu(II) complexes of a *N*,*N*,*O* donor mono-condensed Schiff base ligand: A molecular scaffold forming highly ordered H-bonded rectangular grids. *Inorg. Chim. Acta* **2009**, *362*, 3285–3291. [CrossRef]
59. Liu, X.; Liu, H.; Cen, P.; Chen, X.; Zhou, H.; Song, W.; Hu, Q. Auxiliary ligand-triggered assembly of two dinuclear Cu(II) compounds with a pyridylhydrazone derivative: Synthesis, crystal structure and magnetic property. *Inorg. Chim. Acta* **2016**, *447*, 12–17. [CrossRef]
60. Sarkar, B.; Drew, M.G.B.; Estrader, M.; Diaz, C.; Ghosh, A. Cu^{II} acetate complexes involving *N*,*N*,*O* donor Schiff base ligands: Mono-atomic oxygen bridged dimers and alternating chains of the dimers and $Cu_2(OAc)_4$. *Polyhedron* **2008**, *27*, 2625–2633. [CrossRef]
61. Baggio, R.; Calvo, R.; Garland, M.T.; Peña, O.; Perec, M.; Slep, L.D. A new copper(II) di-μ_2-carboxylato bridged dinuclear complex: $[Cu(oda)phen]_2 \cdot 6H_2O$ (oda = oxydiacetate, phen = phenanthroline). *Inorg. Chem. Commun.* **2007**, *10*, 1249–1252. [CrossRef]

62. Greenaway, A.M.; O'Connor, C.J.; Overman, J.W.; Sinn, E. Magnetic properties and crystal structure of an acetate-bridged ferromagnetic copper(II) dimer. *Inorg. Chem.* **1981**, *20*, 1508–1513. [CrossRef]
63. Bleaney, B.; Bowers, K.D. Anomalous Paramagnetism of Copper Acetate. *Proc. R. Soc. London, Ser. A* **1952**, *214*, 451–465. [CrossRef]